An Induction Flowmeter Insensitive to Asymmetric Flow Profiles

B. Horner and F. Mesch

Institut für Meß- und Regelungstechnik, Universität (TH) Karlsruhe, D-76128 Karlsruhe, Germany

ABSTRACT: As with most of the established flowmeasuring methods, the accuracy of induction flowmeasuring (IFM) is strongly influenced by the shape of the flow profile, so that the flowmeter must be placed sufficiently distant from distorting installations. In many ranges of application this is undesired, difficult or even impossible. In this paper, a novel method for improving the accuracy of induction flowmeters for arbitrary flow profiles is proposed. The accuracy gain is achieved by means of tomographic methods using a set-up consisting of a magnetic field rotating in a plane perpendicular to the flow direction and of multiple electrode pairs. It is shown that errors due to asymmetric profiles become arbitrarily small with growing number of electrodes. Experiments have been carried out with a four-electrode-system and a rotating field subject to asymmetric flow profiles. The experimental results showed a significant improvement in accuracy compared to a conventional two-electrode-system with alternating field.

KEYWORDS: *Induction Flowmeter, Asymmetric Flow, Rotating Field, Multiple Electrodes.*

1. INTRODUCTION

Since the first functional induction flowmeters have been described in the 1930s by *Williams* [1] and *Kolin* [2], great efforts have been made to reduce their inherent sensitivity to flow profiles. After *Thürlemann* [3] had given a first theoretical analysis, *Shercliff* [4] developed a comprehensive theory of induction flowmetering including the derivation of the weight function. The latter in particular helped understanding errors due to distorted flow profiles, because in combination with the exciting magnetic field it assigns a sensitivity to each point in the cross-section of the pipe.

As the flowmeter reading is influenced by the flow velocity field, the exciting magnetic field and the weight function, consequently, three different approaches towards improving the accuracy of induction flowmeters with arbitrary flow profiles have been made, namely manipulation of the magnetic field [5-9], manipulation of the weight function using large electrodes instead of point-shaped ones [10] and (rarely) shaping of the flow profile itself, e.g. by means of a conical inlet [11].

However, neither of these methods is without problems. The use of inhomogeneous instead of uniform magnetic fields generally deteriorates the flowmeter performance with axially symmetric profiles. Also it can be shown, that an ideally inhomogeneous field totally eliminating profile-dependence of the flowmeter cannot exist. Clean large electrodes can smooth the weight function to some degree, but when partially covered with depositions from the liquid they have a varying coupling resistance and yield a randomly distorted weight function. Finally, the shaping of the flow itself is undesired in many cases.

The approach presented in this paper makes use of tomographic methods, which implies measuring more data. However, the additional information thus gained is not used for reconstruction of the flow profile as done in [16,17], but for an improved estimation of the desired parameter, the mean volume flow rate.

2. THEORY

Induction flowmeasuring is based on the Lorentz force acting on moving charge carriers (typically ions) in a flowing liquid due to an externally applied magnetic field. This results in a current field within the liquid,

$$\vec{j}(\vec{x}) = \frac{\vec{v}(\vec{x}) \times \vec{B}(\vec{x})}{\rho(\vec{x})}, \tag{1}$$

where $\vec{v}(\vec{x})$ is the velocity field, $\vec{B}(\vec{x})$ the external magnetic field and $\rho(\vec{x})$ the resistivity of the liquid. The voltage drop of $\vec{j}(\vec{x})$ yields an electric field

$$\vec{E}(\vec{x}) = \vec{v}(\vec{x}) \times \vec{B}(\vec{x}) \tag{2}$$

within the pipe. The electric field can be written as the gradient of a scalar potential $V(\vec{x})$ which is picked up by several electrodes on the pipe wall. Multiplying the Nabla-operator to both sides yields the fundamental equation of the induction flowmeter,

$$\Delta V = \mathrm{div}(\vec{v} \times \vec{B}), \tag{3}$$

where Δ is the Laplacian.

As the aim of this paper is not the detailed presentation of fundamental induction flowmeter theory, only the result for the potential at an arbitrary electrode (index *j*) is given [4,12]:

$$V_j = \iiint_R \vec{W}_j(\vec{x}) \cdot \left(\vec{v}(\vec{x}) \times \vec{B}(\vec{x})\right) d^3x \tag{4}$$

The information about the pipe geometry and the position of the *j*-th electrode is contained in the weight function $\vec{W}_j(\vec{x})$. Assuming a circular pipe and electrodes on the wall, the (two-dimensional) weight function becomes

$$\vec{W}_j(\vec{x}) = \frac{1}{\pi} \cdot \frac{\left(\vec{x} - \vec{\xi}_j\right)}{\left|\vec{x} - \vec{\xi}_j\right|^2} \tag{5}$$

where $\vec{\xi}_j$ is the position of the *j*-th electrode. If a uniform magnetic field is used and the velocity field is only a function of the co-ordinates perpendicular to the pipe axis[1] (corresponding to the *z*-axis here), the problem can be treated in two dimensions. If, in addition, the absence of secondary flow is postulated, a scalar electrode function

[1]Strictly the latter is only true for axially symmetric flow profiles, if the viscosity is not negligible. However, the weight function drops fast outside the electrode plane, thus a velocity profile nearly constant with the axial coordinate *z* can be assumed.

$$\Omega_j(\vec{x}) = \vec{B}_j \int_{-\infty}^{\infty} \vec{W}_j(\vec{x})\, dz \tag{6}$$

can be defined, that represents the differential potential contribution of the points in the electrode plane *C*.

The potential at the *j*-th electrode with the corresponding magnetic field applied can now be written as

$$V_j = \iint_C \Omega_j(\vec{x}) \cdot v(\vec{x})\, d^2x. \tag{7}$$

These potentials are fed into the transducer and processed into a single voltage. This can be described by a transducer function

$$U_T = T(V_1, V_2, \ldots, V_n), \tag{8}$$

where *n* is the number of electrodes. The transducer function can be arbitrarily defined. However, the aim is to find a function that minimises flow profile sensitivity for a given number of electrodes. For an even number of equidistant electrodes this is accomplished, when potential differences between all possible pairs of two opposite electrodes are computed and the results are summed. In a four-electrode-system, for example, as shown in figure 1, the transducer function would be

$$T(V_1, V_2, V_3, V_4) = (V_1 - V_3) + (V_2 - V_4) \tag{9}$$

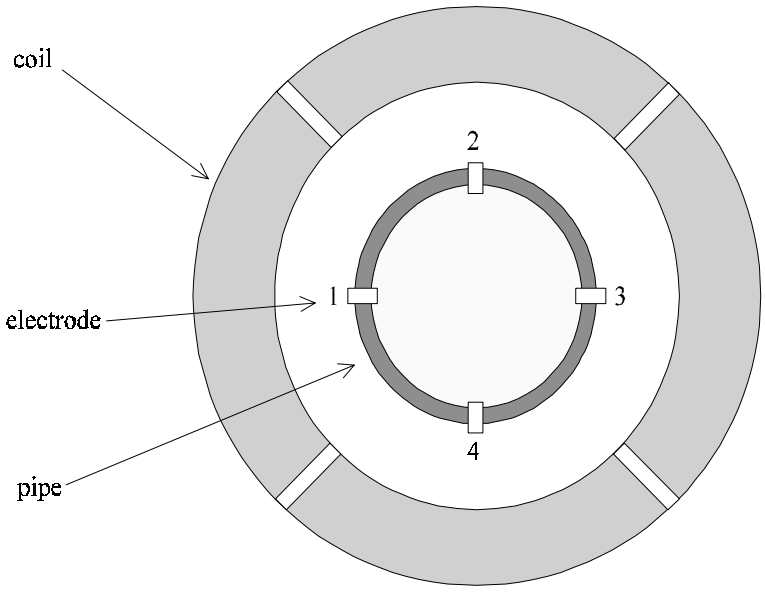

Fig. 1: Schematic cross-section of a four-electrode induction flowmeter.

Inserting the above-defined electrode functions into the four-electrode transducer function (9) yields

$$U_T = \iint_C \Omega_{\text{total}}(\vec{x}) \cdot v(\vec{x})\, d^2x \tag{10}$$

where

$$\Omega_{\text{total},4}(\vec{x}) = \Omega_1(\vec{x}) - \Omega_3(\vec{x}) + \Omega_2(\vec{x}) - \Omega_4(\vec{x}). \tag{11}$$

and

$$\Omega_{\text{total},2}(\vec{x}) = \Omega_1(\vec{x}) - \Omega_3(\vec{x}) \tag{12}$$

for a four- and a two-electrode-system respectively. The latter two functions are depicted below. They have positive singularities at the electrodes and fall with growing distance from the electrodes.

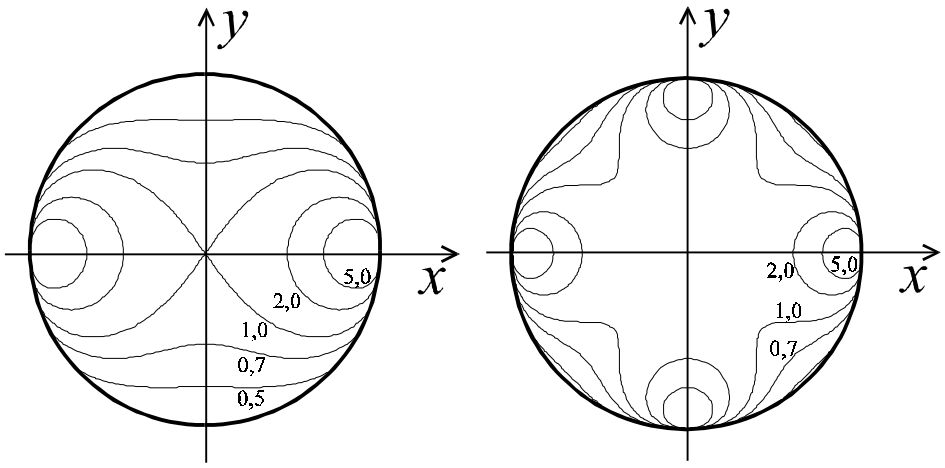

Fig. 2: $\Omega_{\text{total}}(\vec{x})$ of a two- and a four-electrode-system.

For an investigation of a conventional two-electrode system and a four-electrode system regarding accuracy of measurement, it is useful to expand an arbitrary flow profile in polar co-ordinates into a complete system of orthogonal functions and to exploit angular symmetries of the electrode functions [18]. As the flow velocity function $v(r,\varphi)$ is continuous and bounded, Fourier-Bessel-expansion reads

$$v(r,\varphi) = \frac{1}{2}\sum_{s=1}^{\infty} \alpha_{0,s} J_0(\lambda_{0,s} r) + \sum_{n=1}^{\infty}\sum_{s=1}^{\infty} \left(\alpha_{n,s}\cos(n\varphi) + \beta_{n,s}\sin(n\varphi)\right) J_n(\lambda_{n,s} r), \tag{13}$$

with the expansion coefficients

$$\alpha_{n,s} = \frac{2}{\pi J_{n+1}^2(\lambda_{n,s})} \int_0^1 \int_0^{2\pi} v(r,\varphi)\cos(n\varphi) J_n(\lambda_{n,s} r)\, r\, d\varphi\, dr, \tag{14}$$

$$\beta_{n,s} = \frac{2}{\pi J_{n+1}^2(\lambda_{n,s})} \int_0^1 \int_0^{2\pi} v(r,\varphi)\sin(n\varphi) J_n(\lambda_{n,s} r)\, r\, d\varphi\, dr, \tag{15}$$

where $J_n(.)$ is the *n*-th order Bessel-function of the first kind and $\lambda_{n,s}$ its *s*-th positive zero. Eqn. (10) in polar co-ordinates reads

$$U_T = \iint_C \Omega_{\text{total}}(r,\varphi) \cdot v(r,\varphi)\, r\, d\varphi\, dr \tag{16}$$

Insertion of the velocity field expansion (13) into (16) yields:

$$\begin{aligned} U_T = \iint_C \Omega_{\text{total}}(r,\varphi) \cdot \\ \cdot \left[\frac{1}{2} \sum_{s=1}^{\infty} \alpha_{0,s} J_0(\lambda_{0,s} r) + \sum_{n=1}^{\infty} \sum_{s=1}^{\infty} \left(\alpha_{n,s} \cos(n\varphi) + \beta_{n,s} \sin(n\varphi) \right) J_n(\lambda_{n,s} r) \right] r\, dr\, d\varphi . \end{aligned} \tag{17}$$

Multiplication of $\Omega_{\text{total}}(r,\varphi)$ into the outer sum and exchanging the order of summation and integration yields:

$$\begin{aligned} U_T = \frac{1}{2} \iint_C \Omega_{\text{total}}(r,\varphi) \left[\sum_{s=1}^{\infty} \alpha_{0,s} J_0(\lambda_{0,s} r) \right] r\, dr\, d\varphi + \\ + \sum_{n=1}^{\infty} \iint_C \Omega_{\text{total}}(r,\varphi) \cdot \cos(n\varphi) \left[\sum_{s=1}^{\infty} \alpha_{n,s} J_n(\lambda_{n,s} r) \right] r\, dr\, d\varphi + \\ + \sum_{n=1}^{\infty} \iint_C \Omega_{\text{total}}(r,\varphi) \cdot \sin(n\varphi) \left[\sum_{s=1}^{\infty} \beta_{n,s} J_n(\lambda_{n,s} r) \right] r\, dr\, d\varphi \end{aligned} \tag{18}$$

Obviously, the axes of symmetry of $\Omega_{\text{total}}(r,\varphi)$ are the connecting lines of two opposite electrodes and the bisectors between these lines (cf. Fig. 2). For a four-electrode function, this means symmetry at the angles $\varphi = 0, \frac{\pi}{4}, \frac{\pi}{2}, \frac{3\pi}{4}, \pi \ldots$ and for a two-electrode function at the angles $\varphi = 0, \frac{\pi}{2}, \pi, \frac{3\pi}{2} \ldots$, if $\varphi = 0$ at the location of an electrode.

As $\Omega_{\text{total}}(r,\varphi)$ is an even function with regard to φ and $\sin(n\varphi)$ is odd, the third line in eqn. (18) vanishes, because all integrations over an integer number of periods of an odd periodic function yield zero. This result is independent of the number of electrodes. The same argument is not usable for the second line of eqn. (18), because the integrand is even. However, for some values of *n*, the product of $\cos(n\varphi)$ and $\Omega_{\text{total}}(r,\varphi)$ is odd in relation to angles other than $\varphi = 0$. In these cases, the integral also vanishes. It can be shown by simple symmetry considerations, that this is true, if *n* is not a multiple of the number of electrodes. Explicitly, the transducer output U_T contains terms of the orders *n*=0,2,4,6,... for a two-electrode system and terms of the orders *n*=0,4,8,12,... for a four-electrode system, where the first line of eqn. (18) is equivalent to the zero-order term.

As the zero-order term of $v(r,\varphi)$ is independent on φ, it represents the axially symmetric component of the flow. The higher-order terms do not contribute to mean flow velocity, and thus ideally none of these should contribute to the transducer output U_T. However,

only certain higher-order terms are eliminated, depending on the number of electrodes. The remaining higher-order components of the flow contribute to measurement errors.

This means, a four-electrode system eliminates the leading and every second of the higher order disturbance terms as compared with a conventional two-electrode system. Thus, a largely improved accuracy is to be expected for flow velocity profiles deviating from axial symmetry.

3. EXPERIMENTAL SET-UP

To prove the theoretical results, a four-electrode system with a rotating magnetic field has been set up. In order to achieve a homogeneous rotating field, the stator of an induction motor was rewound with two coil pairs of 90° displacement. Pointwise measurement of the resulting magnetic fields with a hall sensor proved uniformity of both magnetic fields within 1% deviation in the electrode plane inside the pipe. The coils were driven by two current-controlled amplifiers fed with 25 Hz sine and cosine. The latter signals were produced by a line-synchronised generator in order to reduce line noise, thus their frequency was exactly half of the line frequency. Rotating magnetic fields of up to 10 mT amplitude could be produced with this set-up.

The sensor was integrated in a perspex pipe of 24 mm inner diameter and 30 mm outer diameter. Four electrodes of 1 mm diameter were placed equidistantly in one plane at the pipe wall. In order to reduce polarisation, the electrodes were gold-plated. An additional ground electrode was provided outside the magnetic field to supply the reference potential. Symmetric electrode cables were used for suppression of induction noise from the coils.

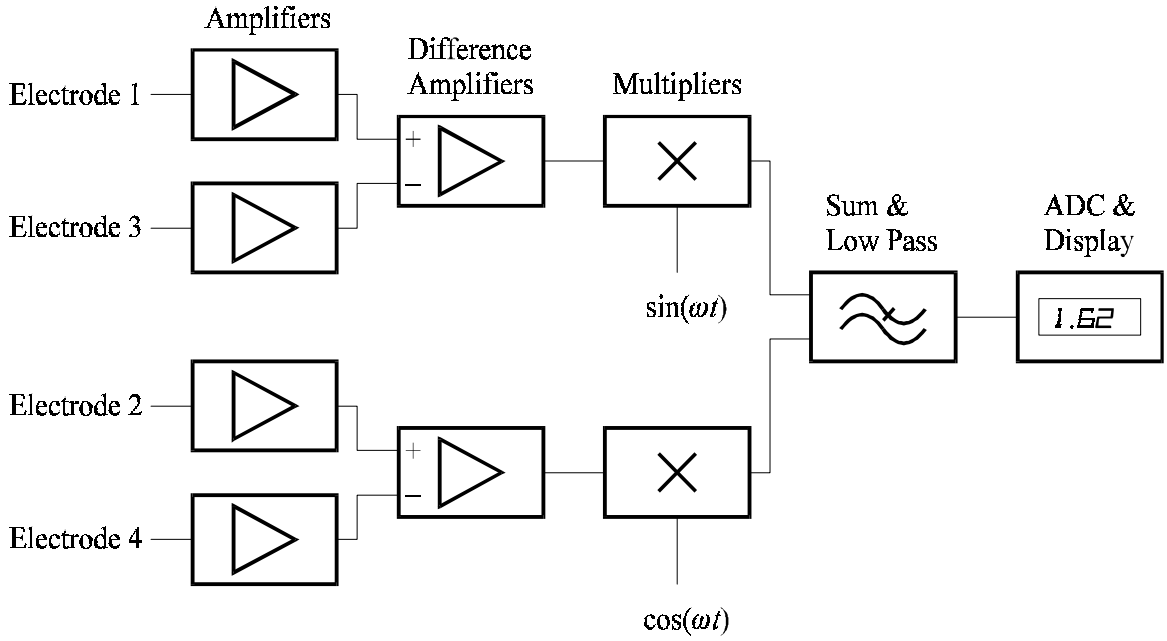

Fig. 3: Schematic diagram of transducer.

The transducer, as depicted in Fig. 3, accepts the electrode potentials (with reference to the ground electrode) as input. The first amplifier stage is equipped with a high pass filter to suppress electrochemical d.c. potentials and is chopper-stabilised to eliminate offset problems. In the next stage, the potentials from opposite electrodes are subtracted. The two difference voltages are then multiplied with a voltage each, which is proportional to the

magnetic field perpendicular to the corresponding electrode axis. At last, the multiplier outputs are added and low-pass-filtered in order to separate the d.c. component. Line noise is suppressed by means of integration over an integer number of periods of the exciting field. This integration is carried out by the ADC stage, and is line-synchronised for high accuracy. The display can be calibrated to arbitrary flowrate units by means of a reference voltage.

For analysis of the performance of the flowmeter described above, it was integrated into a test facility (see Fig. 4) permitting flow velocities of up to 1.8 m/s. From an elevated reservoir, the fluid passed through a relaxation pipe of more than 80 diameters length, then through the flowmeter. For reference, a commercial flowmeter was installed after a relaxation pipe of 30 diameters length behind the experimental flowmeter. Valves enabled exact adjustment of the flowrate.

For purposefully distorting the flow profile and evaluating asymmetry-induced measurement errors, orifices were installed four diameters before the electrode plane. Generally, this leads to a strong deviation from axial symmetry [5]. However, disturbances without swirl component are typically relatively short-lived, so that the commercial reference flowmeter can be expected to be exposed to nearly developed flow.

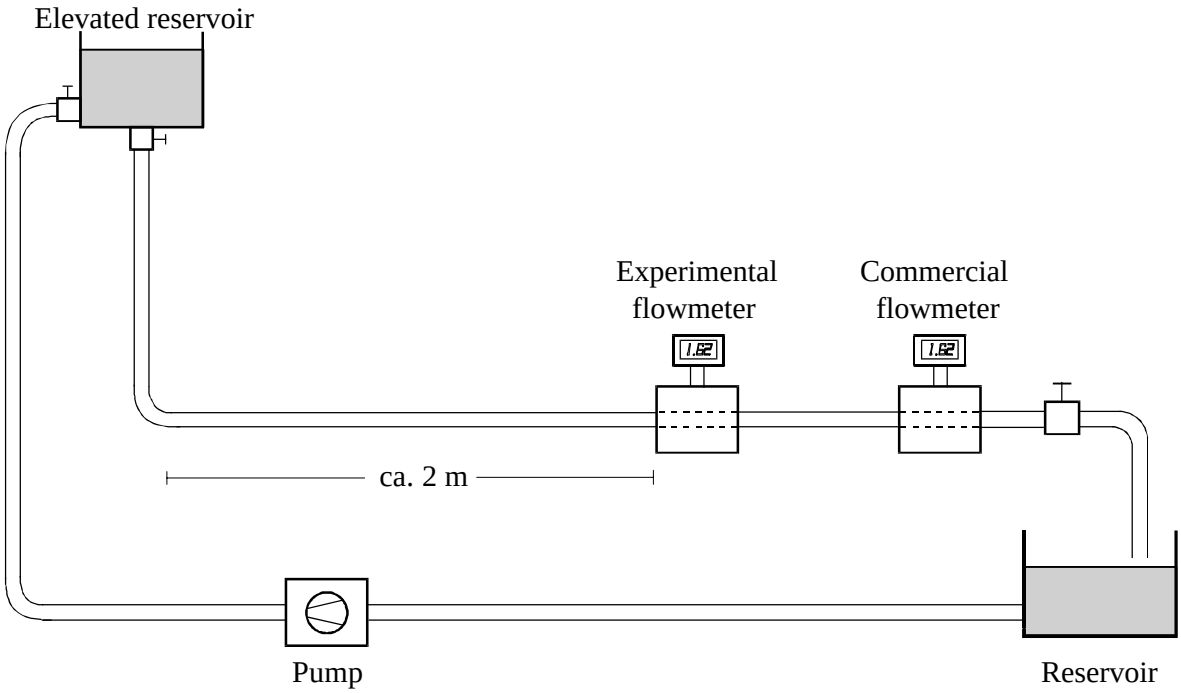

Fig. 4: Flowmeter test facility.

4. MEASUREMENTS

The aim of the measurements was to show that a four-electrode induction flowmeter with rotating magnetic field performs better with distorted profiles than a two-electrode flowmeter. Consequently, the four-electrode data had to be compared with data gathered with a two-electrode system as similar to the four-electrode system as possible. Because the construction principle of the four-electrode flowmeter resembles a set-up of two perpendicular two-electrode flowmeters, this could be easily achieved by disabling one of the excitation coils and evaluating only two electrodes. Thus, only one sensor, one magnet

and one transducer were required for both set-ups, and the results were comparable to a very high degree.

First, both set-ups were calibrated subject to fully developed flow by comparison with the commercial flowmeter integrated in the test facility. As expected, both flowmeters were linear with a statistical measurement error of ca. 0.5% (see Fig. 6a,b). Contained in this value is the measurement uncertainty of the reference flowmeter, which was about 0.2% [13]. After calibration, several different orifices (see Fig. 5) were installed four diameters before the electrode plane of the experimental flowmeter and measurements have been carried out with the four-electrode as well as with the two-electrode set-up. The results were compared with the reading of the reference flowmeter again, which was sufficiently remote from the orifices (30 diameters), so that only slightly distorted flow entered the reference flowmeter.

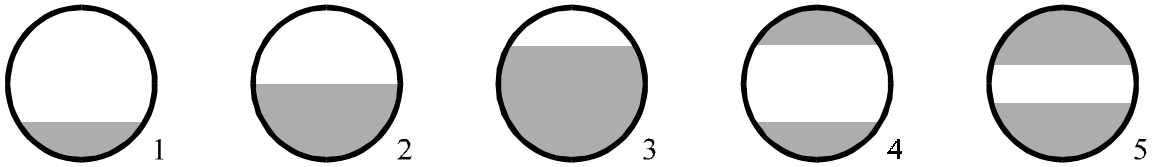

Fig. 5: Flow distortion orifices (grey=solid).
Area fractions: 1: 19,6%, 2: 50%, 3: 80,4%, 4: 39,2% and 5: 68,5%.

The measurement results with the orifices can be grouped as follows: orifice 1 (see Fig. 5) produced results with a measurement error within 0.5% for both set-ups, so obviously the spoiling effect of the distorted profile was too little to be resolved. Orifices 2 and 4 produced errors of approximately 1% with the two-electrode system and ca. 0.7% with the four-electrode system. If the flow profile was heavily distorted, as with the orifices 3 and 5, the performance of the two-electrode system deteriorated extremely, so that typical errors were up to 6% (see Fig. 6c-f). Rotating the orifice by 90° resulted in errors of the same order of magnitude, but with inverse sign. However, the error of the four-electrode system under identical flow conditions was always less than 1%.

5. SUMMARY AND CONCLUSION

Conventional two-electrode induction flowmeters perform precisely with fully developed or only slightly distorted flow. However, they generally fail with heavy distortions, e.g. as caused by bends and valves [5,14,15]. A novel four-electrode induction flowmeter with rotating field has been designed capable of countering those installation effects. Theoretical analysis by means of Fourier-Bessel-expansion showed that errors due to axially asymmetric flow profiles are reduced to a degree depending on the exact structure of the profile. Theoretically, arbitrary accuracy can be achieved with a growing number of electrodes, as long as the flow profile does not change with the axial co-ordinate. The former theoretical results have been verified by experiment. The novel flowmeter described above performs with measurement errors under 1% in flow conditions that cause errors up to 6% with conventional two-electrode meters. Consequently, this technique is particularly suitable for cramped facilities, where installation close to valves or bends can not be avoided. Being realised as an a.c. system here, the same technique is easily adaptable to switched d.c. set-ups. Electrodes, transducers and magnets are either identical to corresponding two-electrode components, or require only minor modifications. Thus, a four-electrode induction flowmeter can easily be set up with industry-standard components, which enables commercial use of this technique.

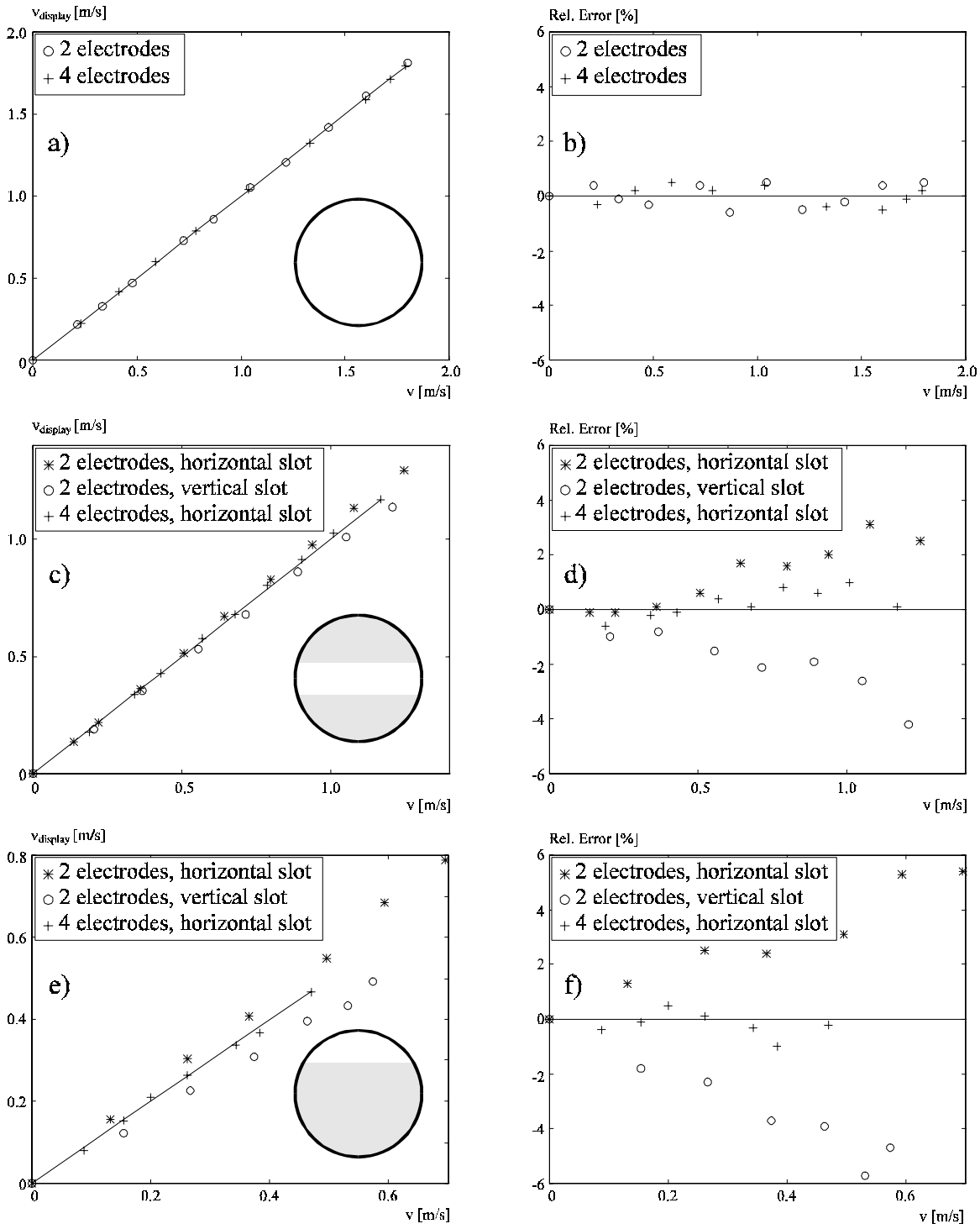

Fig. 6: Measurement results:
a) Measured flow velocity (fully developed flow),
b) Measurement error (fully developed flow),
c) Measured flow velocity (centred slot orifice),
d) Measurement error (centred slot orifice),
e) Measured flow velocity (peripheral slot orifice),
f) Measurement error (peripheral slot orifice).

REFERENCES

[1] E. J. Williams: The induction of electromotive forces in a moving liquid by a magnetic field, and its application to an investigation of the flow of liquids. *Proc. Phys. Soc.* **42** (1930) 466-478.

[2] A. Kolin: An electromagnetic flowmeter. *Proc. Soc. Exp. Biol. Med.* **35** (1936) 53-57.

[3] B. Thürlemann: Methode zur elektrischen Geschwindigkeitsmessung in Flüssigkeiten. *Helv. Phys. Acta* **14** (1941) 383-419.

[4] J. A. Shercliff: The theory of electromagnetic flow-measurement. Cambridge, University Press (1962).

[5] Y. A. Al-Khazraji, R. H. Al-Rabeh, R. C. Baker, J. Hemp: Comparison of the effects of a distorted profile on electromagnetic, ultrasonic and differential pressure flowmeters. *FLOMEKO Groningen* (1978) 215-222.

[6] M. K. Bevir: The theory of induced voltage electromagnetic flowmeters. *J. Fluid Mech.* **43** (1970) 577-590.

[7] J. Hemp: Improved magnetic field for an electromagnetic flowmeter with point electrodes. *J. Phys. D.* **8** (1975) 983-1002.

[8] T. Rummel, B. Ketelsen: Inhomogenes Magnetfeld ermöglicht induktive Durchflußmessung bei allen in der Praxis vorkommenden Strömungsprofilen. *Regelungstechnik.* **14** (1966) 262-267.

[9] W. Engl: Der induktive Durchflußmesser mit inhomogenem Magnetfeld, Parts I & II. *Arch. f. Elektrotechnik.* **53** (1970) 344-359 and **54** (1972) 269-277.

[10] C. C. Smyth: Derivation of weight functions for circular and rectangular channel magnetic flowmeters, by means of Green's theorem and conformal mapping. *J. Phys. E.* **4** (1971) 29-34.

[11] F. Hofmann: Magnetic flowmeter with flowshaping flowtube. *6th FLOMEKO Conference, Seoul/Korea* (1993) 445-451.

[12] G. Schommartz: Induktive Strömungsmessung. VEB Verlag Technik Berlin (1974).

[13] Endress + Hauser: Montage- und Bedienungsanleitung Picomag DMI 6530. (Technical instruction).

[14] J. E. Deacon: Electromagnetic flowmeter installation tests. *3rd FLOMEKO Conference, Budapest/Hungary* (1983) 85-91.

[15] J. E. Halttunen, E. A. Luntta: Modeling in the analysis of installation effects on flowmeters. *6th FLOMEKO Conference, Seoul/Korea* (1993) 174-179.

[16] T. Teshima, S. Honda, Y. Tomita: Electromagnetic flowmeter with multiple poles and electrodes. *Preprint IMTC/94 (IEEE Instr. and Meas. Conf., Shizuoka,* May 1994*).*

[17] Y. Tomita, S. Honda: Estimation of velocity profile by magnetic flowmeter with rotating field. *SICE Conference, Kumamoto/Japan* (1992) 1301-1304.

[18] P. Polly, I. Reinhold: Der Einfluß der Symmetrie-Eigenschaften des Strömungsprofiles beim induktiven Durchflußmesser. *ATM-Blatt* V 1249-14 (1974) 153-158.